HHS Public Access

Author manuscript

Cell Rep. Author manuscript; available in PMC 2016 September 29.

Published in final edited form as:

Cell Rep. 2015 September 29; 12(12): 2099–2110. doi:10.1016/j.celrep.2015.08.049.

TCF1 is required for the T follicular helper cell response to viral infection

Tuoqi Wu[1,*], **Hyun Mu Shin**[2], **E. Ashley Moseman**[3], **Yun Ji**[4], **Bonnie Huang**[1], **Christelle Harly**[4], **Jyoti M. Sen**[5], **Leslie J. Berg**[2], **Luca Gattinoni**[4], **Dorian B. McGavern**[3], and **Pamela L. Schwartzberg**[1,*]

[1]National Human Genome Research Institute, National Institutes of Health, Bethesda, MD, 20892

[2]Department of Pathology, University of Massachusetts Medical School, Worcester, MA 01655

[3]National Institute of Neurological Disorders and Stroke, National Institutes of Health, Bethesda, MD, 20892

[4]National Cancer Institute, National Institutes of Health, Bethesda, MD, 20892

[5]National Institute on Aging, National Institutes of Health, Baltimore, MD, 21224

Summary

T follicular helper (T_{FH}) and Th1 cells generated after viral infections are critical for the control of infection and the development of immunological memory. However, the mechanisms that govern the differentiation and maintenance of these two distinct lineages during viral infection remain unclear. Here, we found that viral-specific T_{FH} and Th1 cells showed reciprocal expression of the transcriptions factors TCF1 and Blimp1 starting early after infection, even before the differential expression of the canonical T_{FH} marker CXCR5. Furthermore, TCF1 was intrinsically required for the T_{FH}-cell response to viral infection; in the absence of TCF1, the T_{FH}-cell response was severely compromised and the remaining TCF1 deficient T_{FH} cells failed to maintain T_{FH}-associated transcriptional and metabolic signatures, which were distinct from those in Th1 cells. Mechanistically, TCF1 functioned through forming negative feedback loops with IL-2 and Blimp1. Our findings demonstrate an essential role of TCF1 in T_{FH}-cell responses to viral infection.

Graphical Abstract

[*]CORRESPONDENCE: NAME: Pamela Schwartzberg and Tuoqi Wu, pams@nhgri.nih.gov; tuoqiwu@gmail.com, Phone: (301) 435-1906, Fax: (301) 402-2170.

The authors declare no competing financial interests.

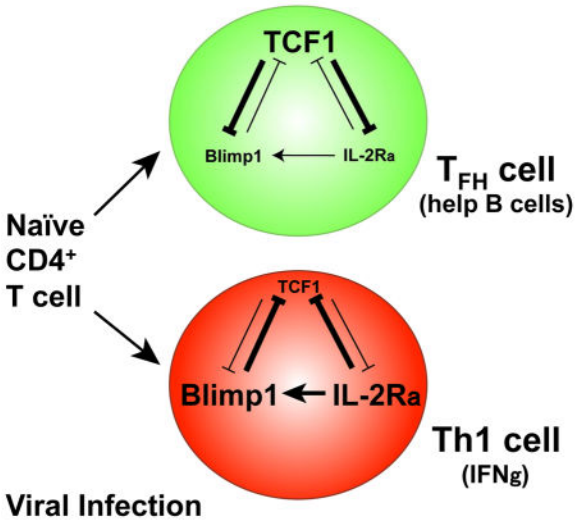

Introduction

CD4 T cells constitute an essential force of the adaptive immune system and are critical for vaccination and immune responses against infections and tumors. CD4 T cells modulate the immune response through various mechanisms, including secretion of cytokines and direct cell-cell interaction. Depending on the antigen, microenvironment, and cytokine milieu, activated CD4 T cells can develop into distinct effector populations, each characterized by unique effector functions and differentiation programming (Crotty, 2011; Zhou et al., 2009). One major function of CD4 T cells is to help the humoral immune response, a function that is carried out by a CD4 subset known as T follicular helper cells (T_{FH} cells) (Cannons et al., 2013; Crotty, 2011). T_{FH} cells express a set of surface markers such as CXCR5, which enable them to migrate to the B-cell follicle and distinguish them from other CD4 subsets. T_{FH} cells provide crucial help for the initiation and maintenance of germinal centers (GC), which are indispensible for antibody affinity maturation and the development of long-term humoral immunity conferred by long-lived plasma cells and memory B cells (Victora and Nussenzweig, 2012). T_{FH} cells signal to antigen presenting cognate B cells through the secretion of cytokines such as IL-4 and IL-21, as well as the expression of CD40L and ICOS that engage their binding partners on B cells (Crotty, 2011).

T_{FH} cells express high levels of Bcl6, a transcriptional repressor, which is essential for T_{FH}-cell differentiation (Johnston et al., 2009; Nurieva et al., 2009; Yu et al., 2009a). In contrast, Blimp1, an antagonist of Bcl6, is highly expressed by non-T_{FH} effector cells and suppresses T_{FH}-cell differentiation (Johnston et al., 2009). Bcl6 expression is triggered in activated T cells early after antigen exposure through the interaction between dendritic cells (DC) and T cells (Baumjohann et al., 2011; Choi et al., 2011). After priming by DCs, T_{FH} cells up-regulate CXCR5, down-regulate CCR7, and move to the T-B zone border where they interact with cognate B cells (Allen et al., 2007; Baumjohann et al., 2011; Haynes et al., 2007). T_{FH} and pre-GC B cells then migrate into the B-cell follicle and initiate the GC reaction (Crotty, 2011). The interaction with cognate B cells is required for maintenance and expansion of T_{FH} cells (Baumjohann et al., 2011; Choi et al., 2011). In contrast, IL-2

signaling restricts the T_{FH}-cell response via STAT5- and Blimp1-mediated pathways (Ballesteros-Tato et al., 2012; Johnston et al., 2012). However, despite recent progress on the regulation of T_{FH}-cell differentiation, many molecular mechanisms involved in the initiation and maintenance of T_{FH} cells remain to be elucidated.

T cell factor 1 (TCF1) is a key transcription factor of the Wnt signaling pathway, which activates Wnt target genes when bound by β-catenin (Verbeek et al., 1995). Multiple TCF1 isoforms are produced as a result of alternative splicing and dual promoter usage of the *Tcf7* gene and can be grouped into long and short isoforms having or lacking the β-catenin binding domain (Van de Wetering et al., 1996). TCF1 is induced by Notch signaling during T cell development and is highly expressed in thymocytes and mature naïve T cells (Xue and Zhao, 2012). Various stages of T cell development, such as T cell lineage commitment of hematopoietic progenitor cells, β-selection, and development from DN to DP thymocytes, are regulated by TCF1 (Germar et al., 2011; Okamura et al., 1998; Weber et al., 2011; Yu et al., 2012). During the CD8 T cell response, TCF1 is required for the development of central memory CD8 T cells and optimal recall response by memory cells (Zhou et al., 2010). In CD4 T cells, TCF1 promotes Th2 differentiation by inducing GATA3 expression and restricts IFNγ expression by Th1 cells (Yu et al., 2009b). However, the role of TCF1 in the T_{FH}-cell differentiation is still unknown.

In this study, we demonstrate that, very early after viral infection, effector CD4 T cells differentiate into TCF1^{high} Blimp1^{low} T_{FH} and TCF1^{low} Blimp1^{high} Th1 cells. Notably, *Tcf7* deficiency led to a T-cell-intrinsic defect in viral-specific T_{FH}-cell responses, associated with decreased T_{FH} cells and reduced GCs. Mechanistically, we find that TCF1 is required for the generation and maintenance of distinct transcriptional and metabolic signatures of T_{FH} cells, including repression of *Il2ra* and *Prdm1*, the gene products of which limit T_{FH}-cell responses. Together, our data demonstrate that TCF1 is essential for the anti-viral T_{FH}-cell response.

Results

Viral-specific effector CD4 T cells can be separated into TCF1^{high} Blimp1^{low} T_{FH} and TCF1^{low} Blimp1^{high} Th1 cells

During viral and intracellular bacterial infections, effector CD4 T cells can be divided into CXCR5^{high} Bcl6^{high} T_{FH} and CXCR5^{low} Blimp1^{high} Th1 cells before the initiation of germinal centers (GC) (Choi et al., 2011; Choi et al., 2013; Pepper et al., 2011). However, it remains unclear how early these two lineages start to diverge. To address this, we used SMARTA CD4 T cells (which express a transgenic TCR that recognizes GP66-77 epitope on lymphocytic choriomeningitis virus (LCMV)) crossed to a Blimp1-YFP reporter to track Blimp1 expression during the response to LCMV (Fooksman et al., 2014; Oxenius et al., 1998). Strikingly, bimodal expression of Blimp1 was observed as early as day 1.5 post-infection (p.i.) (Figures 1A, S1A and S1B), when SMARTA cells had only undergone the first few cell divisions (Figure 1B). Interestingly, at this early timepoint, CXCR5 was expressed by both Blimp1^{high} and Blimp1^{low} cells (Figure 1A). However, after day 2 p.i., Blimp1^{high} SMARTA cells started to express lower levels of CXCR5 than their Blimp1^{low} counterparts (Figure 1A and S1B). Accordingly, analysis of splenic sections from mice

transferred with Blimp1-YFP reporter SMARTA cells revealed that both T_{FH} (Blimp1^{low}) and Th1 (Blimp1^{high}) SMARTA cells could be found in splenic B-cell follicles on day 2 p.i. (Figure S1D). In contrast, by day 3 p.i., most SMARTA cells in B-cell follicles were Blimp1^{low} T_{FH} cells, consistent with the lower expression of CXCR5 in Th1 cells (Figure S1E).

To further characterize the differentiation program of early T_{FH} and Th1 cells, we looked for transcription factors that were differentially expressed between these cells. Based on our unpublished RNA-sequencing studies and previously published data (Choi et al., 2013), T_{FH} cells express much higher levels of *Tcf7* transcripts than their Th1 counterparts. To evaluate this further, we analyzed the kinetics of expression of TCF1, the protein encoded by *Tcf7*, at a single cell level early after LCMV infection by flow cytometry (Figures 1A, 1B, S1A, and S1C). SMARTA T cells could be readily separated into TCF1^{high} and TCF1^{low} populations starting from day 2 p.i., likely as a result of the gradual down-regulation of TCF1 (which is expressed in naïve cells) in a subset of SMARTA cells (Figure 1A and S1A). Notably, whereas TCF1^{high} SMARTA cells maintained high CXCR5, TCF1^{low} SMARTA cells expressed less CXCR5 after day 2 p.i. (Figure 1A and S1C). In addition, there was a clear inverse correlation between TCF1 and Blimp1, as well as a positive correlation between TCF1 and Bcl6 (Figure 1A and S1F), suggesting that TCF1 can be used to distinguish T_{FH} cells from Th1 cells. Indeed, TCF1^{high} SMARTA cells were almost exclusively found in the CXCR5^{high}Blimp1^{low} T_{FH} subset, while TCF1^{low} cells were primarily in the CXCR5^{low}Blimp1^{high} Th1 subset (Figure S1G).

IL-2 signaling suppresses T_{FH} development, and early Th1 cells express more CD25, the high affinity IL-2 receptor, than early T_{FH} cells (Ballesteros-Tato et al., 2012; Choi et al., 2011; Johnston et al., 2012; Pepper et al., 2011). We found that while most SMARTA cells showed substantial CD25 expression on day 1.5 p.i., TCF1^{high} T_{FH} cells down-regulated CD25 much faster than TCF1^{low} Th1 cells (Figure S1F). We also found that expression of Tim3, a co-inhibitory receptor expressed by exhausted CD8 T cells (Jin et al., 2010; Sakuishi et al., 2010), correlated well with Blimp1 (Figure S1F). We therefore used Tim3 as an early Th1 marker when the Blimp1-YFP reporter was not available.

To determine whether the dichotomy of Blimp1 and TCF1 expression between T_{FH} and Th1 cells was maintained later during infection when T_{FH}-cell responses rely on antigen presentation by GC B cells (Baumjohann et al., 2011; Choi et al., 2011), we examined their expression in SMARTA cells one week after LCMV infection. As expected, CXCR5^{high} T_{FH} cells mostly expressed low levels of Blimp1 (Figure 1C and S1H) and SLAM (Figure S1I) (Johnston et al., 2009). Strikingly, TCF1 still negatively correlated with Blimp1 expression; co-staining of TCF1 and Blimp1 clearly separated SMARTA into two populations (Figure 1C and S1H). Furthermore, TCF1^{high} cells were again primarily in the CXCR5^{high}Blimp1^{low} T_{FH} population, while the CXCR5^{low}Blimp1^{high} cells contained mostly TCF1^{low} cells (Figure S1J) in which TCF staining was only slightly higher than that in B cells, which do not express TCF1 (Staal and Clevers, 2000) (Figure 1C). *Tcf7* encodes multiple isoforms as a result of alternative splicing and dual promoter usage (Van de Wetering et al., 1996). The flow cytometry antibody we used binds to the N-terminal β-catenin binding domain, and therefore only recognizes the long isoforms. To further

evaluate TCF1 expression, we sorted T_{FH} and Th1 SMARTA cells on day 3 p.i. and day 8 p.i. and evaluated TCF1 protein levels by immunoblots using an antibody that recognizes all isoforms. While T_{FH} cells from both timepoints expressed multiple isoforms with or without the β-catenin binding domain, expression of all TCF1 isoforms was very low in Th1 cells, particularly on day 3 p.i. (Figure 1D). Thus, TCF1 protein levels are high in T_{FH} but low in Th1 cells in both pre-GC phase and GC phase of the immune response to LCMV.

Tcf7 is repressed by IL-2 and Blimp1

The bifurcation in *Tcf7* expression between T_{FH} and Th1 cells prompted us to investigate which signals induce the loss of *Tcf7* in Th1 cells. IL-2 signaling suppresses T_{FH} differentiation and Bcl6 expression in activated CD4 T cells (Ballesteros-Tato et al., 2012; Johnston et al., 2012; Oestreich et al., 2012). The fact that $TCF1^{low}$ Th1 cells expressed more CD25, the high affinity IL-2 receptor, than $TCF1^{high}$ T_{FH} cells (Figure S1F), suggested IL-2 might suppress *Tcf7*. To examine this possibility, we monitored the effect of IL-2 on *in vitro* activated CD4 T cells. We stimulated CD4 T cells with anti-CD3ε and CD28 for 3 days, then washed and cultured cells with or without IL-2 for one additional day. CD4 T cells receiving IL-2 expressed higher surface CD25, consistent with the role of IL-2 in promoting CD25 expression. Moreover, these cells expressed 50% less TCF1 than cells cultured without IL-2 (Figure 2A). Thus, differential IL-2 signals between T_{FH} and Th1 cells may contribute to differences in TCF1 levels.

A previous study suggested that IL-2 suppresses T_{FH} differentiation via Blimp1 (Johnston et al., 2012). The inverse correlation between TCF1 and Blimp1 expression suggested that Blimp1 might also selectively repress the *Tcf7* locus in Th1 cells. To examine this possibility, we transduced SMARTA cells with retroviral vectors expressing a scrambled shRNA or shRNA targeting *Prdm1*, which encodes Blimp1, and analyzed the effect on TCF1 levels in Th1 cells. Knock down of Blimp1 caused an increase of TCF1 expression in $CXCR5^{low}CD25^{high}$ Th1 SMARTA cells on day 3 p.i., compared to untransduced or control vector transduced Th1 SMARTA cells (Figure 2B). Interestingly, the region 30kb upstream of the *Tcf7* transcription start site (TSS) (Figure S2) contains evolutionarily conserved sequences with Blimp1 binding motifs (GAAAG) (Kuo and Calame, 2004). This region is bound by TCF1 itself, as well as other transcription factors based on published chromatin-immunoprecipitation-sequencing (ChIP-seq) data from different cell types and has been shown to regulate *Tcf7* transcription (Germar et al., 2011; Steinke et al., 2014; Wu et al., 2012). Indeed, using ChIP assays, we found that Blimp1 physically interacted with this region in T_{FH} and Th1 SMARTA cells (Figure 2C); however, the binding of Blimp1 was significantly stronger in Th1 cells than in T_{FH} cells, consistent with the different abundance of Blimp1 in the two populations. We also observed more H3 K4 trimethylation (H3K4me3), which is associated with active transcription (Jenuwein and Allis, 2001), in this region in T_{FH} cells than in Th1 cells, while more H3 K27 trimethylation (H3K27me3), which is linked to transcriptional repression (Cao et al., 2002), was found in Th1 cells than T_{FH} cells (Figure 2D). Furthermore, the -30kb region increased luciferase activity by 2-fold relative to a control luciferase construct; however, over-expression of Blimp1 repressed the enhancer activity of this region (Figure 2E). Thus, Blimp1 may suppress *Tcf7* expression in Th1 cells.

Tcf7 deficiency causes a severe defect in the T_{FH}-cell response to LCMV

The high expression of TCF1 in T_{FH} cells suggested a potential role of TCF1 in T_{FH}-cell development. *Tcf7* is a key player in multiple steps during T cell development (Verbeek et al., 1995; Weber et al., 2011). To study the immune response of mature T cells, we bred mice carrying a conditional *Tcf7* allele to CD4-Cre mice, which initiate Cre activity in DP thymocytes (Steinke et al., 2014), to generate *Tcf7* conditional (cKO) mice. Cre-mediated deletion caused more than 10-fold reduction in TCF1 in CD4 T cells (Figure S3A). Although naïve cKO mice had lower CD4 T cell frequencies than WT controls, frequencies of $CD44^{high}$ CD4 T cells were comparable (Figure S3B). We then infected cKO and WT mice with LCMV and analyzed LCMV-specific CD4 T cell responses using the GP66-77 IA^b tetramer on day 10 p.i.. We used CXCR5, PD1, and Bcl6 to stain T_{FH} cells and SLAM to stain Th1 cells. While the ratio of $CXCR5^{high}$ $SLAM^{low}$ T_{FH} to $CXCR5^{low}$ $SLAM^{high}$ Th1 $tetramer^+$ CD4 T cells was close to 1 in WT mice, the frequency of T_{FH} cells among $tetramer^+$ cells in cKO mice was markedly decreased (Figure 3A). We also observed a substantial loss of $tetramer^+$ $CXCR5^{high}$ $PD1^{high}$ and $CXCR5^{high}Bcl6^{high}$ GC-T_{FH} populations in cKO mice. Accordingly, the number of GP66-77-specific T_{FH} cells in the spleens of cKO mice was reduced by more than 6-fold (Figure 3B). In contrast, the numbers of GP66-77-specific Th1 cells were not significantly different between cKO and WT mice. TCF1 levels in GP66-77-specific CD4 T cells were substantially decreased, even in the remaining $CXCR5^+$ T_{FH} cells, suggesting that the small fraction of T_{FH} cells in cKO mice was not likely caused by incomplete recombination (Figure S3C). Moreover, defective T_{FH}-cell responses in cKO mice were not unique to one epitope, as the frequencies of T_{FH} cells among total $CD44^{high}$ CD4 T cells and total T_{FH} counts in cKO spleens were also reduced (Figure 3C). Consistent with the role of T_{FH} cells in supporting humoral responses and GC formation (Crotty, 2011), the numbers of GC ($GL7^{high}$ FAS^{high}) B cells and activated (IgD^{low} FAS^{high}) B cells in the cKO mice were less than half of those in WT mice (Figure 3D).

To rule out that loss of TCF1 during thymocyte development compromised T_{FH} differentiation in cKO mice, we crossed the conditional *Tcf7* to ERT2-Cre mice, which activate Cre by tamoxifen treatment (Seibler et al., 2003). By treating the inducible *Tcf7* knockout mice (iKO) with tamoxifen for several days immediately prior to LCMV infection, we ensured that iKO T cells had undergone thymic development similar to their ERT2-Cre^{neg} counterparts (data not shown). Similar to cKO mice, T_{FH}-cell responses in tamoxifen treated iKO mice on day 10 p.i. were severely compromised compared to vehicle-treated counterparts, confirming that *Tcf7* is critical for T_{FH}-cell responses during LCMV infection (Figure 3E).

T_{FH} cells require TCF1 in a CD4 T cell autonomous manner

In the above experiments, TCF1 was deleted in both CD4 and CD8 T cells in cKO and iKO mice. To determine whether defective T_{FH}-cell responses in *Tcf7* KO mice were intrinsic to CD4 T cells, we crossed *Tcf7* cKO mice to SMARTA mice. Congenically marked naïve CD4 T cells from WT and cKO SMARTA mice were isolated, mixed at 1:1 ratios, and adoptively transferred to WT CD45.1 mice, which were subsequently infected with LCMV (Figure 4A). By mixing WT and cKO SMARTA cells, we could compare the two within

each recipient exposed to the same exact conditions and determine their phenotype with higher accuracy and sensitivity. T_{FH} cell differentiation involves an early B-cell-independent phase and a subsequent B-cell-dependent phase (Baumjohann et al., 2011; Choi et al., 2011). To investigate the impact of *Tcf7* deficiency on each phase of T_{FH} differentiation, we monitored CD4 T cell responses on day 3 and 8 p.i.. On day 3 p.i., loss of TCF1 preferentially reduced T_{FH}-cell responses as evidenced by the decreased frequencies of $CXCR5^{high}$ $Tim3^{low}$ as well as $CXCR5^{high}Bcl6^{high}$ cells among cKO SMARTA cells (Figures 4B, 4C, and S4B). *Tcf7* deficiency also caused a reduction in the number of T_{FH} ($CXCR5^{high}$ $Tim3^{low}$) SMARTA cells and, to a lesser extent, the number of Th1 ($CXCR5^{low}$ $Tim3^{high}$) SMARTA cells (Figure S4C). We then monitored the differentiation of SMARTA cells at the peak of the immune response (day 8 p.i.) and observed an even more profound loss of T_{FH} cells in cKO SMARTA cells compared to that on day 3 p.i.. The frequencies of $CXCR5^{high}$ $SLAM^{low}$ cells (Figure 4D) and $CXCR5^{high}Bcl6^{high}$ cells (Figures 4E and S4E) were 4~5 fold lower in cKO cells than those in their WT counterparts. Similarly, there was close to a 10 fold reduction in the numbers of cKO T_{FH} SMARTA cells compared to those of WT, yet no significant difference between the numbers of cKO and WT Th1 cells (Figure S4F).

To delete TCF1 only in naive SMARTA cells, we generated *Tcf7* iKO SMARTA mice and transferred mixed naive SMARTA CD4 T cells from iKO SMARTA mice and their ERT2-Cre^{-} counterparts (WT SMARTA) to WT recipients, which then were treated with tamoxifen followed by LCMV infection. Similar to cKO SMARTA cells, induced deletion of TCF1 preferentially affected T_{FH} responses: Both the frequencies and numbers of T_{FH} ($CXCR5^{high}$ $Tim3^{low}$ or $CXCR5^{high}Bcl6^{high}$) iKO SMARTA cells on day 3 p.i. were lower than their WT counterparts (Figure S4H, S4I, and S4J). Again, on day 8 p.i., we observed greater reductions in the frequencies and numbers of T_{FH} ($CXCR5^{high}$ $SLAM^{low}$ or $CXCR5^{high}Bcl6^{high}$) cells (Figures 4F, 4G, S4L) within the iKO SMARTA population, yet Th1 cell numbers were similar to WT (Figure S4M). Together, our results demonstrate a cell-intrinsic requirement for TCF1 for viral-specific T_{FH}-cell responses.

Finally, to further evaluate the capacity of *Tcf7*-deficient CD4 T cells to support humoral responses, we adoptively transferred equal numbers of WT or iKO SMARTA CD4 T cells separately into SAP KO mice, which can not generate GC responses due to defects in CD4 help (Crotty et al., 2003; Qi et al., 2008), treated the chimeras with tamoxifen, and then infected them with LCMV. On day 11 p.i., B-cell responses were determined by the numbers of GC ($GL7^{high}$ FAS^{high}) and activated (IgD^{low} FAS^{high}) B cells. In SAP KO mice that received iKO SMARTA cells, the numbers of both GC and activated B cells were lower than those that received WT cells (Figure 4H). Thus, T-cell intrinsic defects caused by the loss of TCF1 led to a compromised humoral response.

Tcf7 deficiency directly compromises T_{FH}-cell expansion

To determine how *Tcf7* deficiency affects T_{FH} cells, we examined the proliferative capacity of cKO SMARTA cells, as determined by their incorporation of Bromodeoxyuridine (BrdU). Interestingly, loss of TCF1 caused a reduction in BrdU incorporation in T_{FH} but not Th1 cKO SMARTA cells on day 5 p.i., at the middle of the clonal expansion phase (Figure

S4N). Moreover, cKO T_{FH} cells showed slightly stronger annexin V staining than their WT counterparts, suggesting that cKO T_{FH} cells may be more prone to apoptosis (Figure S4O). To directly compare the ability of *Tcf7*-deficient and sufficient T_{FH} cells to expand, we sorted WT and iKO T_{FH} (CXCR5^{high} Tim3^{low}) and Th1 (CXCR5^{low} Tim3^{high}) SMARTA cells on day 3 p.i., mixed equal numbers of WT and iKO T_{FH} or WT and iKO Th1 SMARTA cells, and transferred the mixed T_{FH} or Th1 cells into infection-matched recipients. Four days post-transfer (day 7 p.i.), ~80% of the progeny from both WT and iKO donor T_{FH} cells stayed as T_{FH} cells (CXCR5^{high} SLAM^{low}), while a slightly higher percentage of progeny from iKO donor Th1 cells stayed as Th1 cells than those from WT donor Th1 cells (Figure S4P snd S4Q). However, the numbers of progeny from iKO donor T_{FH} cells were only half the numbers from WT donor T_{FH} cells, suggesting that *Tcf7* deficiency indeed compromised the expansion of the transferred T_{FH} cells, likely as a result of reduced proliferation and/or survival.

Transcriptomic analyses of *Tcf7* deficient T_{FH} and Th1 cells

To gain further insights into the properties of *Tcf7* deficient T_{FH} and Th1 cells as well as the molecular pathways regulated by TCF1 in these cells, we set up adoptive transfers and infections as described in Figure 4A, and performed microarray experiments to profile the transcriptomes of WT and cKO T_{FH} and Th1 SMARTA cells sorted from the same mice on day 8 p.i.. As the proportion of T_{FH} cells was much lower among cKO SMARTA cells than their WT counterparts, we compared the transcriptomes between WT and cKO cells within the T_{FH} or Th1 subset in order to filter out genes that were differentially expressed simply due to the reduced T_{FH}:Th1 ratio caused by *Tcf7* deficiency. We first generated T_{FH} and Th1 signature gene sets by listing genes that were ≥2-fold ($p<0.05$) more expressed in day 8 p.i. WT T_{FH} cells than day 8 p.i. WT Th1 cells or vice versa (Table S1). Then, we used gene set enrichment analysis (GSEA) (Subramanian et al., 2005) to determine whether these signatures were enriched in cKO cells or WT cells. Strikingly, day 8 cKO SMARTA T_{FH} cells exhibited reduced T_{FH} gene expression signatures and increased Th1 signatures compared to WT SMARTA T_{FH} cells (Figure 5A).

To better understand pathways affected by *Tcf7* deficiency, we performed GSEA to compare the gene signatures of cKO and WT T_{FH} cells using Kyoto Encyclopedia of Genes and Genomes (KEGG) and Reactome curated pathway databases. cKO T_{FH} cells showed significantly reduced signatures related to gene expression (e.g. basal transcription factors, spliceosome, aminoacyl-tRNA biosynthesis), DNA repair (e.g. nucleotide excision repair), cell cycle and metabolism (e.g. valine, leucine and isoleucine degradation, pentose phosphate pathway, fatty acid metabolism, citrate cycle) (Table S2 and S3). The reduced signatures related to branched-chain amino acids degradation, fatty acid degradation and the citrate cycle in cKO T_{FH} cells (Figure 5B) prompted us to investigate whether *Tcf7* deficiency affected mitochondria in T_{FH} cells. Using MitoTracker Green FM to quantify the mitochondrial mass in SMARTA cells, we found that WT T_{FH} cells had higher mitochondrial mass than WT Th1 cells (Figure 5C), suggesting there were metabolic differences between Th1 and T_{FH} cells. Notably, we also observed that mitochondrial mass was reduced in cKO SMARTA T_{FH} cells and to a lesser extent in cKO SMARTA Th1 cells (Figure 5D). The intensity of DiOC6(3) staining in cells can be used to measure

mitochondrial membrane potential, an indicator of mitochondrial function (Rottenberg and Wu, 1998). Again, we found that WT T_{FH} cells showed stronger DiOC6(3) staining than WT Th1 cells (Figure 5E). However, both T_{FH} and Th1 cKO SMARTA cells showed less DiOC6(3) staining than their WT counterparts (Figure 5F). Together, our data suggest that T_{FH} cells exhibit metabolic differences from Th1 cells, and furthermore that *Tcf7*-deficient T_{FH} cells lose these characteristic properties of T_{FH} cells. Thus, TCF1 appears to be required to generate and/or maintain T_{FH} identity during viral infection.

TCF1 negatively regulates the expression of CD25 and Blimp1

Among the genes up-regulated in cKO T_{FH} cells (Table S4), were *Prdm1* and *Il2ra*, which encode Blimp1 and CD25, two proteins involved in pathways that suppress T_{FH}-cell differentiation. QRT-PCR results confirmed that *Prdm1* and *Il2ra* transcripts in *Tcf7* deficient T_{FH} cells were higher than those in WT T_{FH} cells on day 3 as well as day 8 p.i. (Figures 6A and 6B). The elevated *Il2ra* transcript and surface CD25 levels (Figure S5A) in *Tcf7* deficient T_{FH} cells suggested a potential increase in IL-2 responsiveness. To address this, we cultured WT and cKO SMARTA cells isolated on day 5 p.i. with or without IL-2 and measured IL-2 signaling by staining phosphorylated-STAT5 (pSTAT5). pSTAT5 levels were higher in T_{FH} cKO SMARTA cells than in their WT counterparts (Figure 6C), indicating elevated IL-2 signaling in T_{FH} cKO cells.

Published TCF1 ChIP-seq data from both thymocytes (Germar et al., 2011) and mature CD8 T cells (Steinke et al., 2014) indicate the presence of TCF1 binding peaks in the third intron of *Prdm1* as well as the first intron of *Il2ra* and a region 23kb upstream of *Il2ra* TSS (Figures S5B, S5C, and S5D); the region in the third intron of *Prdm1* has been shown to be important for *Prdm1* expression in other cell types (Tunyaplin et al., 2004). To test whether TCF1 physically interacts with these regions in viral-specific CD4 T cells, we performed TCF1 ChIP experiments on sorted T_{FH} and Th1 SMARTA cells. Strikingly, TCF1 bound strongly to all three regions in T_{FH} cells but not in Th1 cells (Figure 6D). Moreover, these TCF1 binding sites showed extensive H3K27me3 modification, associated with transcriptional repression (Cao et al., 2002), in T_{FH} cells but not in Th1 cells (Figure S5E). Thus, TCF1 can bind *Prdm1* and *Il2ra* in T_{FH} cells, and loss of TCF1 leads to abnormal up-regulation of these genes in T_{FH} cells.

Rescue of *Tcf7*-deficient phenotype by enforced expression of Bcl6

Our results showed that TCF1 in T_{FH} cells suppresses the expression of *Prdm1* (Figure 6). Given that Blimp1, encoded by *Prdm1*, can be antagonized by Bcl6 (Crotty, 2011), we reasoned that over-expression of Bcl6 might rescue the defective T_{FH}-cell differentiation caused by loss of TCF1. To test this hypothesis, we over-expressed Bcl6 in WT or cKO SMARTA cells through retroviral transduction (Figure 7A). On day 8 p.i., enforced expression of Bcl6 rectified the defective T_{FH}-cell differentiation in cKO SMARTA cells, greatly increasing the T_{FH} frequency of cKO SMARTA cells (Figure 7B). Thus, TCF1 acts upstream of the Bcl6-Blimp1 axis to regulate T_{FH}-cell responses.

Discussion

Upon viral or intracellular bacterial infections, effector CD4 T cells differentiate into Th1 cells, which protect the host through secreted cytokines such as IFNγ and TNFα and/or direct lysis of infected cells, and T_{FH} cells, which provide help for B-cell responses (Choi et al., 2011; Crotty, 2011; Pepper et al., 2011; Swain et al., 2012). The differentiation of T_{FH} and Th1 cells occurs before GC initiation and depends on DC priming and ICOS-ICOSL interactions between activated CD4 T cells and DCs (Choi et al., 2011; Pepper et al., 2011). However, the molecular mechanisms that govern and maintain the balance of these two distinct subsets are still unclear. TCF1 is critical for thymic T cell development as well as Th2 polarization and the development of memory CD8 T cells during immune responses (Weber et al., 2011; Yu et al., 2009b; Zhou et al., 2010). Here, we have shown that viral-specific T_{FH} cells maintain high levels of TCF1, while viral-specific Th1 cells down-regulate TCF1 early after infection. We further show that both IL-2 and Blimp1 lead to TCF1 downregulation. Importantly, TCF1 was intrinsically required for robust antiviral T_{FH}-cell responses as well as T cell help to B cells; in the absence of TCF1, we observed decreased numbers of T_{FH} cells and germinal center B cells and the remaining *Tcf7* deficient T_{FH} cells exhibited reduced T_{FH} cell transcriptional and metabolic signatures. We further provide evidence that TCF1 also acts upstream of the Blimp1-Bcl6 axis and suppresses expression of both *Prdm1* and *Il2ra*, the products of which suppress T_{FH} differentiation.

Previous studies have shown that induction of Bcl6 and CXCR5 is associated with early T_{FH} cells, while up-regulation of Blimp1 and CD25 is associated with early Th1 cells (Baumjohann et al., 2011; Choi et al., 2011; Pepper et al., 2011). However, the precise timing and details of the mechanisms involved in the commitment of the two lineages remains obscure. In this study, we demonstrate that the pre-GC phase of effector CD4 T cell differentiation can be further divided into two stages. In the first stage, viral-specific CD4 T cells differentiate into either $TCF1^{high}$ $Blimp1^{low}$ T_{FH} or $TCF1^{low}$ $Blimp1^{high}$ Th1 cells. The two subsets expressed similar levels of CXCR5 and both could be found in B-cell follicles at this stage. In the second stage, Th1 cells lost CXCR5 expression and were now excluded from B-cell follicles. Interestingly, early T_{FH} cells down-regulated CD25 rapidly and expressed high levels of *Tcf7*, closely resembling early memory precursor CD8 T cells (Arsenio et al., 2014; Kalia et al., 2010). These cells also have a transcriptional signature similar to memory precursors (Choi et al., 2013). Of note, a subset of $CXCR5^{+}$ memory CD4 T cells have been found in the circulation of both human and mice, reiterating a potential shared regulatory network between early viral-specific T_{FH} cells and early memory precursors (He et al., 2013; Locci et al., 2013). It is interesting to speculate that TCF1 may be a component in this shared signaling network, given its critical role in the development of memory CD8 T cells (Zhou et al., 2010). Indeed, loss of TCF1 caused a profound defect in the T_{FH}-cell response to viral infection, as shown here and by two other recent studies (Choi et al., 2015; Xu et al., 2015). It worth noting, however, that, in our hands, the loss of T_{FH} cells in *Tcf7* deficient SMARTA cells on day 3 p.i. was less dramatic than that on day 8 p.i.. It is possible that while TCF1 is required for optimal T_{FH}-cell responses prior to GC formation, a redundant mechanism, such as the expression of the related transcription factor LEF1, may compensate for *Tcf7* deficiency during T_{FH} differentiation (Choi et al., 2015).

However, we also found evidence for both reduced proliferation and reduced cell survival of TCF1-deficient T_{FH} cells between day 3 and day 7 p.i., which is a major part of the clonal expansion phase. Thus, TCF1 may be required for the full expansion of T_{FH} cells, which may account for the differences in the extent of T_{FH} defects between day 3 and day 8 p.i.. It should also be noted that although we have not found evidence of conversion from *Tcf7* deficient T_{FH} cells to Th1 cells after tracking them for several days in infection-matched mice, we did see a reduction in T_{FH} gene expression and metabolic signatures in the absence of TCF1. TCF1 can also suppress expression of the Th1 cytokine IFNγ. Thus, TCF1 may be critical both for T_{FH} expansion/survival and for the generation and maintenance of T_{FH} identity in the face of strong Th1-inducing signals as seen in viral infections. In this respect, it is of interest that we have not seen a requirement for TCF1 for T_{FH} responses during protein immunization with alum as an adjuvant, which is considered a Th2-inducing condition (TW, unpublished data).

Previous studies have suggested that signaling mediated by CD25 and Blimp1, which are abundantly expressed in early Th1 cells, inhibit T_{FH}-cell differentiation (Choi et al., 2011; Johnston et al., 2012; Pepper et al., 2011). Our ChIP and gene expression profiles of *Tcf7* deficient T_{FH} cells suggest that TCF1 potentially represses expression of *Prdm1* and *Il2ra*. Indeed, CD25 expression was lost much faster in T_{FH} cells than in Th1 cells early after infection. Given the high levels of TCF1 in T_{FH} cells, TCF1 may contribute to their rapid loss of CD25. Furthermore, since IL-2 signaling increases CD25 expression, this could amplify IL-2 signaling in Th1 cells, generating a positive feedback loop that may contribute to the difference in CD25 expression between the two subsets. It is of note that two recent papers have found that loss of TCF1 or both TCF1 and LEF1 led to reduced Bcl6 as well as increased Blimp1 expression in T_{FH} cells (Choi et al., 2015; Xu et al., 2015). While we did not observe decreased Bcl6 expression, we did find that overexpression of Bcl6 rescues T_{FH} cell generation in the absence of TCF1, confirming that TCF1 acts upstream of the Blimp1/Bcl6 axes. Moreover, we found that TCF1 not only represses Blimp1 and CD25 expression, but also is repressed by Blimp1 and IL2, suggesting that TCF1 is a critical component of negative feedback loops with IL-2 and Blimp1 that may regulate the differentiation and maintenance of T_{FH} cells during viral infections.

Upon antigen encounter, T cells switch from oxidative phosphorylation to aerobic glycolysis, a pattern that is enforced in Th1 cells by IL-2 (MacIver et al., 2013; Oestreich et al., 2014). However, the metabolic profile of T_{FH} cells remains largely unknown. We found that T_{FH} cells have greater mitochondrial mass than Th1 cells. An enhanced mitochondrial mass was also observed in memory T cells, which is correlated with elevated fatty acid oxidation (van der Windt et al., 2012). Interestingly, our gene expression profiling data showed that *Tcf7* deficient T_{FH} cells had reduced gene expression signatures related to branched amino acid degradation, fatty acid degradation, and the citrate cycle, suggesting reduced oxidative metabolism. Consistent with these findings, the loss of TCF1 led to reduced mitochondrial mass and function in T_{FH} cells. Thus, TCF1 may contribute to the regulation of T_{FH} cell metabolism and promote a more oxidative metabolic profile, although additional studies will be necessary to determine potential targets of TCF1 that contribute to these processes and whether they influence T_{FH}-cell differentiation.

In summary, our study has demonstrated that the distinct high levels of TCF1 expression distinguish T_{FH} cells from Th1 cells and are critical for the development of viral-specific T_{FH} cells. In addition, we have identified potential negative feedback loops linking TCF1 to IL-2 and Blimp1. Our findings unveil an essential role of TCF1 in contributing to the balance between immune responses mediated by two major CD4 subsets during viral infection and may help shed light on pathways important for the development of vaccines and immune therapies targeting viral infections.

Experimental Procedures

Mice and infections

Tcf7 conditional mice (*Tcf7*$^{tm1a(EUCOMM)Wtsi}$, Institut Clinique de la Souris) were crossed to Flp Deleter (Taconic, 7089), and either CD4-Cre (Lee et al., 2001) or ERT2-Cre (Seibler et al., 2003) (Taconic) to generate *Tcf7*$^{loxP/loxP}$; CD4-Cre (cKO) or *Tcf7*$^{loxP/loxP}$; ERT2-Cre (iKO) mice, and to SMARTA transgenic mice, expressing a TCR recognizing the LCMV GP66-77 epitope (Oxenius et al., 1998). Blimp1-YFP mice (Fooksman et al., 2014) were crossed to SMARTA mice. Other mouse strains, in vitro activation, retroviral transduction, flow cytometry, microscopy, RNA and protein analyses, chromatin immunoprecipitation and luciferase assays are described in online supplemental material. For adoptive transfers, 10^6 (for day 1.5, 2, and 3) or 10^4 (for other timepoints) SMARTA CD4 T cells were transferred to recipient mice, unless indicated. Mice were intravenously (i.v.) injected with 2×10^6 (for day 1.5, 2, and 3) or 2×10^5 (for other timepoints) plaque-forming unit (PFU) of LCMV Armstrong. For ERT2-Cre inducible knockouts, 2mg tamoxifen in corn oil was injected intraperitoneally (i.p.) daily for 3~5 d before LCMV infection. Controls were either Cre^- mice or mice transferred with ERT2-Cre^- SMARTA injected with Tamoxifen or ERT2-Cre^+ animals injected with vehicle. All animal husbandry and experiments were approved by the NHGRI or NINDS Animal Use and Care Committees.

Accession Numbers

Microarray data have been uploaded to GEO (accession # GSE65660). Link: http://www.ncbi.nlm.nih.gov/geo/query/acc.cgi?token=wzadkuwqndiddix&acc=GSE65660.

Statistical analysis

Two-tailed paired or unpaired Student's t-test was performed with GraphPad Prism 6 to calculate p values. *p<0.05, **p<0.01, ***p<0.001, ****p<0.0001.

Supplementary Material

Refer to Web version on PubMed Central for supplementary material.

Acknowledgments

We thank J. Reilley, R. Handon, M. Kirby, S. Anderson, and E. Stregevsky for excellent technical support. This work was supported by funds from the intramural programs of NHGRI, NINDS, NCI, NIA as well as NIH grant AI101048 (LJB).

References

Allen CD, Okada T, Cyster JG. Germinal-center organization and cellular dynamics. Immunity. 2007; 27:190–202. [PubMed: 17723214]

Arsenio J, Kakaradov B, Metz PJ, Kim SH, Yeo GW, Chang JT. Early specification of CD8+ T lymphocyte fates during adaptive immunity revealed by single-cell gene-expression analyses. Nature immunology. 2014; 15:365–372. [PubMed: 24584088]

Ballesteros-Tato A, Leon B, Graf BA, Moquin A, Adams PS, Lund FE, Randall TD. Interleukin-2 inhibits germinal center formation by limiting T follicular helper cell differentiation. Immunity. 2012; 36:847–856. [PubMed: 22464171]

Baumjohann D, Okada T, Ansel KM. Cutting Edge: Distinct waves of BCL6 expression during T follicular helper cell development. Journal of immunology. 2011; 187:2089–2092.

Cannons JL, Lu KT, Schwartzberg PL. T follicular helper cell diversity and plasticity. Trends in immunology. 2013; 34:200–207. [PubMed: 23395212]

Cao R, Wang L, Wang H, Xia L, Erdjument-Bromage H, Tempst P, Jones RS, Zhang Y. Role of histone H3 lysine 27 methylation in Polycomb-group silencing. Science. 2002; 298:1039–1043. [PubMed: 12351676]

Choi YS, Gullicksrud JA, Xing S, Zeng Z, Shan Q, Li F, Love PE, Peng W, Xue HH, Crotty S. LEF-1 and TCF-1 orchestrate T differentiation by regulating differentiation circuits upstream of the transcriptional repressor Bcl6. Nature immunology. 2015 Published online 27 July 2015.

Choi YS, Kageyama R, Eto D, Escobar TC, Johnston RJ, Monticelli L, Lao C, Crotty S. ICOS receptor instructs T follicular helper cell versus effector cell differentiation via induction of the transcriptional repressor Bcl6. Immunity. 2011; 34:932–946. [PubMed: 21636296]

Choi YS, Yang JA, Yusuf I, Johnston RJ, Greenbaum J, Peters B, Crotty S. Bcl6 expressing follicular helper CD4 T cells are fate committed early and have the capacity to form memory. Journal of immunology. 2013; 190:4014–4026.

Crotty S. Follicular helper CD4 T cells (TFH). Annual review of immunology. 2011; 29:621–663.

Crotty S, Kersh EN, Cannons J, Schwartzberg PL, Ahmed R. SAP is required for generating long-term humoral immunity. Nature. 2003; 421:282–287. [PubMed: 12529646]

Fooksman DR, Nussenzweig MC, Dustin ML. Myeloid cells limit production of antibody-secreting cells after immunization in the lymph node. Journal of immunology. 2014; 192:1004–1012.

Germar K, Dose M, Konstantinou T, Zhang J, Wang H, Lobry C, Arnett KL, Blacklow SC, Aifantis I, Aster JC, Gounari F. T-cell factor 1 is a gatekeeper for T-cell specification in response to Notch signaling. Proceedings of the National Academy of Sciences of the United States of America. 2011; 108:20060–20065. [PubMed: 22109558]

Haynes NM, Allen CD, Lesley R, Ansel KM, Killeen N, Cyster JG. Role of CXCR5 and CCR7 in follicular Th cell positioning and appearance of a programmed cell death gene-1high germinal center-associated subpopulation. Journal of immunology. 2007; 179:5099–5108.

He J, Tsai LM, Leong YA, Hu X, Ma CS, Chevalier N, Sun X, Vandenberg K, Rockman S, Ding Y, et al. Circulating precursor CCR7(lo)PD-1(hi) CXCR5(+) CD4(+) T cells indicate Tfh cell activity and promote antibody responses upon antigen reexposure. Immunity. 2013; 39:770–781. [PubMed: 24138884]

Jenuwein T, Allis CD. Translating the histone code. Science. 2001; 293:1074–1080. [PubMed: 11498575]

Jin HT, Anderson AC, Tan WG, West EE, Ha SJ, Araki K, Freeman GJ, Kuchroo VK, Ahmed R. Cooperation of Tim-3 and PD-1 in CD8 T-cell exhaustion during chronic viral infection. Proceedings of the National Academy of Sciences of the United States of America. 2010; 107:14733–14738. [PubMed: 20679213]

Johnston RJ, Choi YS, Diamond JA, Yang JA, Crotty S. STAT5 is a potent negative regulator of TFH cell differentiation. The Journal of experimental medicine. 2012; 209:243–250. [PubMed: 22271576]

Johnston RJ, Poholek AC, DiToro D, Yusuf I, Eto D, Barnett B, Dent AL, Craft J, Crotty S. Bcl6 and Blimp-1 are reciprocal and antagonistic regulators of T follicular helper cell differentiation. Science. 2009; 325:1006–1010. [PubMed: 19608860]

Kalia V, Sarkar S, Subramaniam S, Haining WN, Smith KA, Ahmed R. Prolonged interleukin-2Ralpha expression on virus-specific CD8+ T cells favors terminal-effector differentiation in vivo. Immunity. 2010; 32:91–103. [PubMed: 20096608]

Kuo TC, Calame KL. B lymphocyte-induced maturation protein (Blimp)-1, IFN regulatory factor (IRF)-1, and IRF-2 can bind to the same regulatory sites. Journal of immunology. 2004; 173:5556–5563.

Lee PP, Fitzpatrick DR, Beard C, Jessup HK, Lehar S, Makar KW, Perez-Melgosa M, Sweetser MT, Schlissel MS, Nguyen S, et al. A critical role for Dnmt1 and DNA methylation in T cell development, function, and survival. Immunity. 2001; 15:763–774. [PubMed: 11728338]

Locci M, Havenar-Daughton C, Landais E, Wu J, Kroenke MA, Arlehamn CL, Su LF, Cubas R, Davis MM, Sette A, et al. Human circulating PD-1+CXCR3−CXCR5+ memory Tfh cells are highly functional and correlate with broadly neutralizing HIV antibody responses. Immunity. 2013; 39:758–769. [PubMed: 24035365]

MacIver NJ, Michalek RD, Rathmell JC. Metabolic regulation of T lymphocytes. Annual review of immunology. 2013; 31:259–283.

Nurieva RI, Chung Y, Martinez GJ, Yang XO, Tanaka S, Matskevitch TD, Wang YH, Dong C. Bcl6 mediates the development of T follicular helper cells. Science. 2009; 325:1001–1005. [PubMed: 19628815]

Oestreich KJ, Mohn SE, Weinmann AS. Molecular mechanisms that control the expression and activity of Bcl-6 in TH1 cells to regulate flexibility with a TFH-like gene profile. Nature immunology. 2012; 13:405–411. [PubMed: 22406686]

Oestreich KJ, Read KA, Gilbertson SE, Hough KP, McDonald PW, Krishnamoorthy V, Weinmann AS. Bcl-6 directly represses the gene program of the glycolysis pathway. Nature immunology. 2014; 15:957–964. [PubMed: 25194422]

Okamura RM, Sigvardsson M, Galceran J, Verbeek S, Clevers H, Grosschedl R. Redundant regulation of T cell differentiation and TCRalpha gene expression by the transcription factors LEF-1 and TCF-1. Immunity. 1998; 8:11–20. [PubMed: 9462507]

Oxenius A, Bachmann MF, Zinkernagel RM, Hengartner H. Virus-specific MHC-class II-restricted TCR-transgenic mice: effects on humoral and cellular immune responses after viral infection. European journal of immunology. 1998; 28:390–400. [PubMed: 9485218]

Pepper M, Pagan AJ, Igyarto BZ, Taylor JJ, Jenkins MK. Opposing signals from the Bcl6 transcription factor and the interleukin-2 receptor generate T helper 1 central and effector memory cells. Immunity. 2011; 35:583–595. [PubMed: 22018468]

Qi H, Cannons JL, Klauschen F, Schwartzberg PL, Germain RN. SAP-controlled T-B cell interactions underlie germinal centre formation. Nature. 2008; 455:764–769. [PubMed: 18843362]

Rottenberg H, Wu S. Quantitative assay by flow cytometry of the mitochondrial membrane potential in intact cells. Biochimica et biophysica acta. 1998; 1404:393–404. [PubMed: 9739168]

Sakuishi K, Apetoh L, Sullivan JM, Blazar BR, Kuchroo VK, Anderson AC. Targeting Tim-3 and PD-1 pathways to reverse T cell exhaustion and restore anti-tumor immunity. The Journal of experimental medicine. 2010; 207:2187–2194. [PubMed: 20819927]

Seibler J, Zevnik B, Kuter-Luks B, Andreas S, Kern H, Hennek T, Rode A, Heimann C, Faust N, Kauselmann G, et al. Rapid generation of inducible mouse mutants. Nucleic acids research. 2003; 31:e12. [PubMed: 12582257]

Staal FJ, Clevers H. Tcf/Lef transcription factors during T-cell development: unique and overlapping functions. The hematology journal: the official journal of the European Haematology Association/EHA. 2000; 1:3–6. [PubMed: 11920163]

Steinke FC, Yu S, Zhou X, He B, Yang W, Zhou B, Kawamoto H, Zhu J, Tan K, Xue HH. TCF-1 and LEF-1 act upstream of Th-POK to promote the CD4(+) T cell fate and interact with Runx3 to silence CD4 in CD8(+) T cells. Nature immunology. 2014; 15:646–656. [PubMed: 24836425]

Subramanian A, Tamayo P, Mootha VK, Mukherjee S, Ebert BL, Gillette MA, Paulovich A, Pomeroy SL, Golub TR, Lander ES, Mesirov JP. Gene set enrichment analysis: a knowledge-based approach for interpreting genome-wide expression profiles. Proceedings of the National Academy of Sciences of the United States of America. 2005; 102:15545–15550. [PubMed: 16199517]

Swain SL, McKinstry KK, Strutt TM. Expanding roles for CD4(+) T cells in immunity to viruses. Nature reviews Immunology. 2012; 12:136–148.

Tunyaplin C, Shaffer AL, Angelin-Duclos CD, Yu X, Staudt LM, Calame KL. Direct repression of prdm1 by Bcl-6 inhibits plasmacytic differentiation. Journal of immunology. 2004; 173:1158–1165.

Van de Wetering M, Castrop J, Korinek V, Clevers H. Extensive alternative splicing and dual promoter usage generate Tcf-1 protein isoforms with differential transcription control properties. Molecular and cellular biology. 1996; 16:745–752. [PubMed: 8622675]

van der Windt GJ, Everts B, Chang CH, Curtis JD, Freitas TC, Amiel E, Pearce EJ, Pearce EL. Mitochondrial respiratory capacity is a critical regulator of CD8+ T cell memory development. Immunity. 2012; 36:68–78. [PubMed: 22206904]

Verbeek S, Izon D, Hofhuis F, Robanus-Maandag E, te Riele H, van de Wetering M, Oosterwegel M, Wilson A, MacDonald HR, Clevers H. An HMG-box-containing T-cell factor required for thymocyte differentiation. Nature. 1995; 374:70–74. [PubMed: 7870176]

Victora GD, Nussenzweig MC. Germinal centers. Annual review of immunology. 2012; 30:429–457.

Weber BN, Chi AW, Chavez A, Yashiro-Ohtani Y, Yang Q, Shestova O, Bhandoola A. A critical role for TCF-1 in T-lineage specification and differentiation. Nature. 2011; 476:63–68. [PubMed: 21814277]

Xu L, Cao Y, Xie Z, Huang Q, Bai Q, Yang X, He R, Hao Y, Wang H, Zhao T, et al. The transcription factor TCF-1 initiates the differentiation of T cells during acute viral infection. Nature immunology. 2015 Published online 27 July 2015.

Xue HH, Zhao DM. Regulation of mature T cell responses by the Wnt signaling pathway. Annals of the New York Academy of Sciences. 2012; 1247:16–33. [PubMed: 22239649]

Yu D, Rao S, Tsai LM, Lee SK, He Y, Sutcliffe EL, Srivastava M, Linterman M, Zheng L, Simpson N, et al. The transcriptional repressor Bcl-6 directs T follicular helper cell lineage commitment. Immunity. 2009a; 31:457–468. [PubMed: 19631565]

Yu Q, Sharma A, Oh SY, Moon HG, Hossain MZ, Salay TM, Leeds KE, Du H, Wu B, Waterman ML, et al. T cell factor 1 initiates the T helper type 2 fate by inducing the transcription factor GATA-3 and repressing interferon-gamma. Nature immunology. 2009b; 10:992–999. [PubMed: 19648923]

Yu S, Zhou X, Steinke FC, Liu C, Chen SC, Zagorodna O, Jing X, Yokota Y, Meyerholz DK, Mullighan CG, et al. The TCF-1 and LEF-1 transcription factors have cooperative and opposing roles in T cell development and malignancy. Immunity. 2012; 37:813–826. [PubMed: 23103132]

Zhou L, Chong MM, Littman DR. Plasticity of CD4+ T cell lineage differentiation. Immunity. 2009; 30:646–655. [PubMed: 19464987]

Zhou X, Yu S, Zhao DM, Harty JT, Badovinac VP, Xue HH. Differentiation and persistence of memory CD8(+) T cells depend on T cell factor 1. Immunity. 2010; 33:229–240. [PubMed: 20727791]

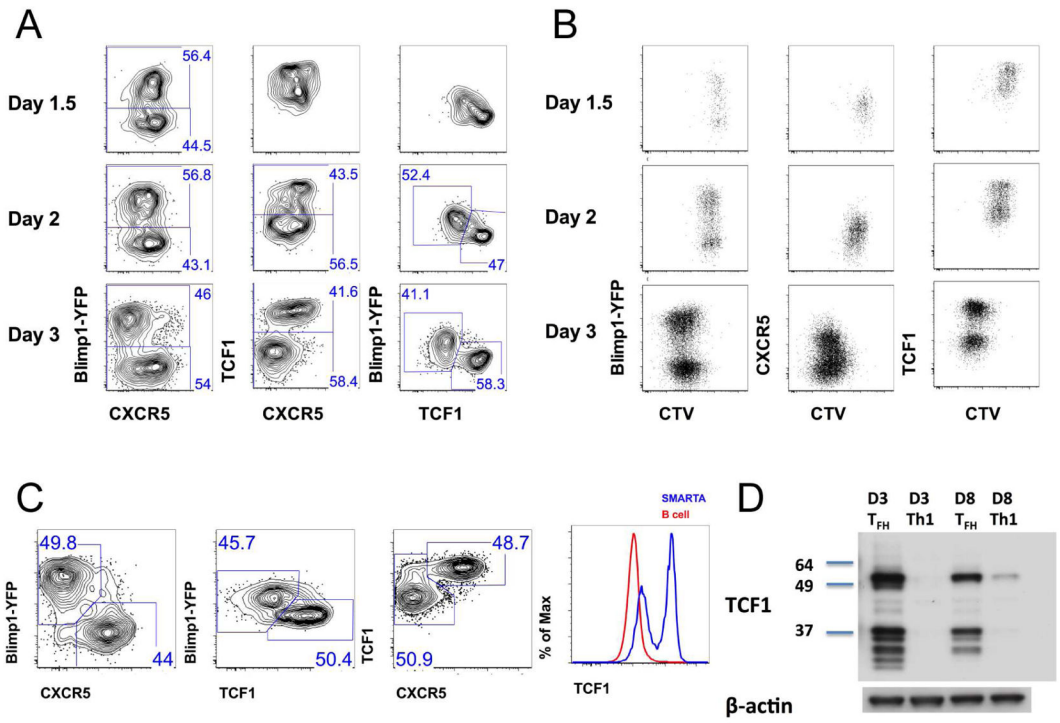

Figure 1. TCF1 is differentially expressed between T_{FH} and Th1 cells after LCMV infection

(A, B) 10^6 CellTrace™ Violet labeled (CTV) purified naïve CD45.1$^+$ Blimp1-YFP SMARTA CD4 T cells were transferred into C57BL/6 mice followed by infection with LCMV Armstrong. Splenocytes (gated on CD45.1$^+$ SMARTA CD4 T cells) were analyzed on day 1.5, 2, and 3 after infection. (A) Analyses of Blimp1-YFP, CXCR5, and TCF1 expression. (B) Analyses of CTV dilution plus phenotypic markers. (C) C57BL/6 mice received 10^4 purified naïve CD45.1$^+$ Blimp1-YFP SMARTA CD4 T cells and were infected with LCMV Armstrong. Splenocytes (gated on SMARTA cells) were analyzed on day 7 p.i., for Blimp1-YFP, CXCR5, and TCF1. Right: TCF1 in SMARTA cells (blue) and host B cells (red). (D) TCF1 protein in day 3 T_{FH} (CXCR5^{high}Tim3^{low}), day 3 Th1 (CXCR5^{low}Tim3^{high}), day 8 T_{FH} (CXCR5^{high}SLAM^{low}), and day 8 Th1 (CXCR5^{low}SLAM^{high}) SMARTA CD4 T cells. β-actin was used as a loading control. Data in (A, B) are from a single experiment (n≥2 per timepoint), representative of >4 independent experiments. Data in (C) are from a single experiment (n=3) representative of 2 independent experiments. Western blots are representative of 2 independent experiments.

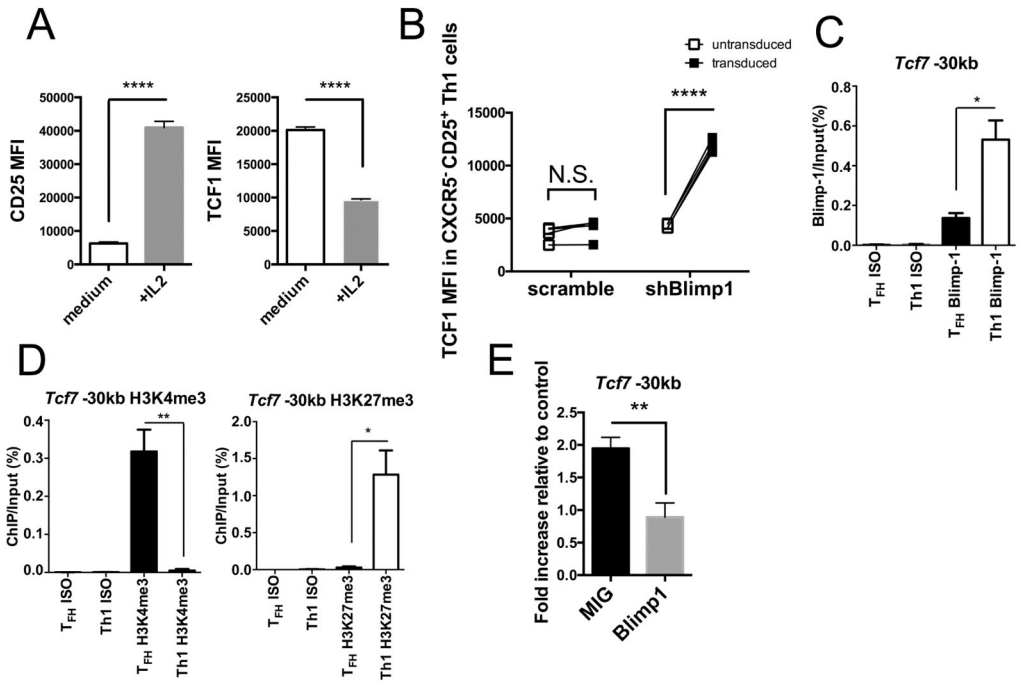

Figure 2. IL-2 and Blimp1 negatively regulate TCF1 expression

(A) Naïve CD4 T cells were stimulated with anti-CD3 and anti-CD28 for 3 days, then cultured with or without hIL-2 for 1 day and the mean fluorescence intensity (MFI) of CD25 and TCF1 determined by flow cytometry. Unpaired Student's t tests were performed; error bars represent SD. Data are from a single experiment representative of 4 independent experiments. (B) 10^6 SMARTA CD4 T cells were transduced with retroviruses containing a scrambled control sequence or shRNA for *Prdm1*, and transferred into C57BL/6 recipients followed by infection with LCMV. On day 3 p.i., TCF1 expression in Th1 ($CXCR5^{low}CD25^{high}$) SMARTA cells was determined. Paired Student's t tests were performed between transduced (GFP^+) and untransduced populations within each group. Each line represents data from one individual mouse. Data are from a single experiment (n=4 per group) representative of 2 independent experiments. (C, D) Day 8 p.i., T_{FH} and Th1 SMARTA T cells were isolated and ChIP assays performed with antibodies to Blimp-1 (C) or a control IgG, and with antibodies to modified histone H3 (D) as indicated. ChIPs were amplified by QRT-PCR for the indicated region. Data are the mean +/− SEM of three independent experiments. Significance was determined by an unpaired t test. (E) 293T cells were co-transfected with pGL3 SV40 promoter vector containing *Tcf7* −30kb region and MSCV-IRES-GFP (MIG) with or without Blimp1. Luciferase activity was normalized to Renilla activity and adjusted to the fold increase over empty pGL3 SV40 vector. Data are the mean +/− SD of three independent transfections in one of 2 independent experiments. Significance was determined by an unpaired t test.

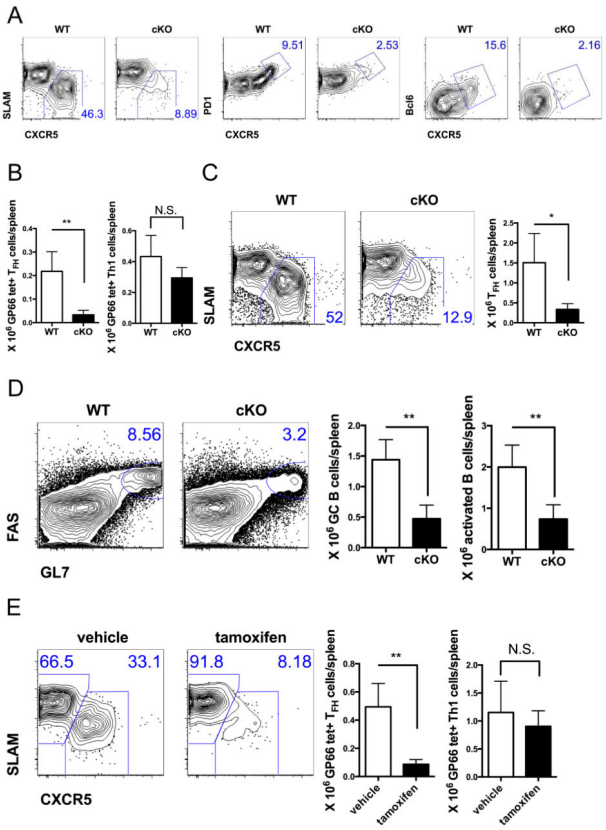

Figure 3. TCF1 is required for the differentiation of T_{FH} cells

(A–D) *Tcf7*$^{loxP/loxP}$; CD4-Cre (cKO) mice and littermate controls (WT) were infected with LCMV and splenocytes isolated on day 10 p.i.. (A) Analyses of CXCR5, SLAM, PD1, and Bcl6 in WT and cKO GP66-77 IA^b tetramer$^+$ CD4 T cells. (B) Numbers of GP66-77 IA^b tetramer$^+$ CXCR5^{high}SLAM^{low} (T_{FH}) and CXCR5^{low}SLAM^{high} (Th1) CD4 T cells in spleens of WT or cKO mice. (C) Representative FACS plots of CXCR5 and SLAM staining (gated on CD44^{high} CD4 T cells) and numbers of CXCR5^{high}SLAM^{low}CD44^{high} (T_{FH}) CD4 T cells in spleens. (D) Representative FACS plots and numbers of FAS^{high}GL7^{high} (GC) B cells (gated on CD19$^+$B220$^+$ cells) and activated (IgD^{low} FAS^{high}) B cells in WT and cKO spleens. (E) *Tcf7*$^{loxP/loxP}$; ERT2-Cre (iKO) mice were treated with either 2mg tamoxifen or vehicle daily for 3 days and then infected with LCMV. Day 10 p.i. analyses of CXCR5 and SLAM staining (gated on GP66-77 IA^b tetramer$^+$ CD4 T cells) and numbers of GP66-77 IA^b tetramer$^+$ CXCR5^{high}SLAM^{low} (T_{FH}) and CXCR5^{low}SLAM^{high} (Th1) CD4 T cells in the spleens. Data in (A–D) are from a single experiment (n=4 per genotype), representing 2 independent experiments. Data in (E) are from a single experiment (n=4 per genotype), representative of 3 independent experiments. Significance was determined by unpaired t tests; error bars represent SD.

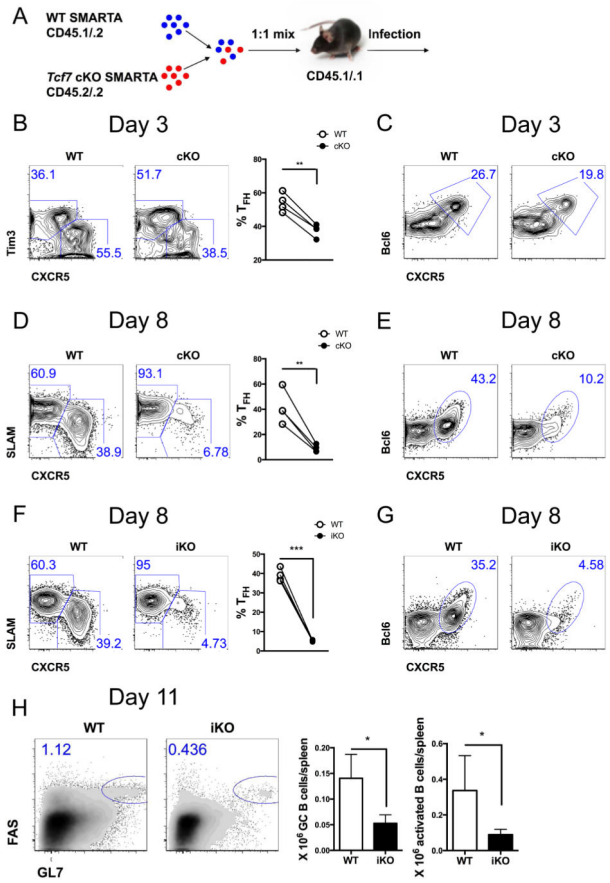

Figure 4. Loss of TCF1 causes a cell-intrinsic defect in T_{FH} cell differentiation starting from early after infection

(A–E) Purified CD4 T cells from cKO ($CD45.1^{-}CD45.2^{+}$) and WT ($CD45.1^{+}CD45.2^{+}$) SMARTA mice were mixed at ~1:1 ratio, transferred into WT CD45.1 mice (10^6 cells per recipient for day 3 and 10^4 cells for day 8 experiments). Chimeras were then infected with LCMV. TCF1 deletion was confirmed by flow cytometry (Figure S4A, S4D). Data are from a single experiment (n=4) representative of 3 independent experiments. Each line represents data from one mouse. (B, C) Frequencies of T_{FH} ($CXCR5^{high}$ $Tim3^{low}$ or $CXCR5^{high}Bcl6^{high}$) and Th1 ($CXCR5^{low}$ $Tim3^{high}$) cells in WT and cKO SMARTA cells in spleens on day 3 p.i.. (D, E) Frequencies of T_{FH} ($CXCR5^{high}$ $SLAM^{low}$ or $CXCR5^{high}Bcl6^{high}$) and Th1 ($CXCR5^{low}$ $SLAM^{high}$) cells in splenic WT and cKO SMARTA cells on day 8 p.i.. (F, G) Purified CD4 T cells from iKO ($CD45.1^{-}CD45.2^{+}$) and WT ($CD45.1^{+}CD45.2^{+}$) SMARTA mice were mixed at ~1:1 ratio and transferred into WT CD45.1 mice, which were then treated with 2mg tamoxifen for 3 days. Chimeras were then infected with LCMV and analyzed on 8 day p.i. for TCF1 (Figure S4K), and for frequencies of T_{FH} ($CXCR5^{high}$ $SLAM^{low}$ or $CXCR5^{high}Bcl6^{high}$) and Th1 ($CXCR5^{low}$ $SLAM^{high}$) cells in WT and iKO SMARTA cells. Data are from a single experiment (n=4) representative of 3 independent experiments. Each line represents data from one mouse. (H) SAP KO ($CD45.2^{-}$) mice were transferred with 5000 purified CD4 T cells from iKO or WT SMARTA ($CD45.2^{+}$) mice, treated with 2mg tamoxifen daily for 3 days, infected with

LCMV and splenocytes stained for GC ($GL7^{high}$ FAS^{high}) B cells and activated (IgD^{low} FAS^{high}) B cells on day 11p.i.. Flow plots were gated on $CD19^{+}B220^{+}$ cells. Data are from a single experiment (n=4) representative of 3 independent experiments. Statistical significance was determined by paired (B–G) or unpaired (H) t tests; error bars represent SD.

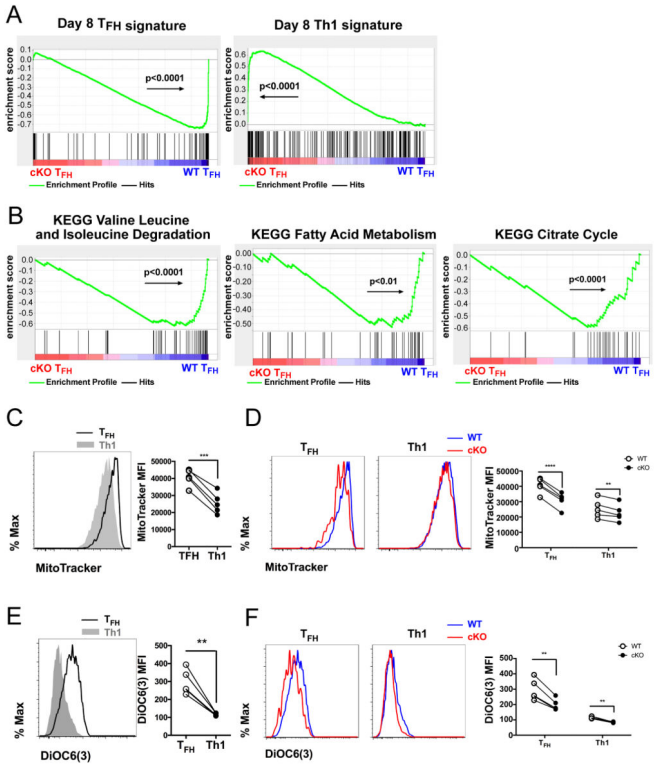

Figure 5. Loss of TCF1 changes the transcriptional and metabolic signatures of T_{FH} cells

(A) Microarray analyses of day 8 T_{FH} (CXCR5^{high} SLAM^{low}) and Th1 (CXCR5^{low} SLAM^{high}) cKO and WT SMARTA cells isolated by cell sorting from co-transfer experimnets setup as in Figure 4A. Genes expressed >2-fold ($p<0.05$) in WT T_{FH} cells than WT Th1 cells were listed as the T_{FH} gene set and those >2-fold ($p<0.05$) expressed in WT Th1 cells were listed as the Th1 gene set (Table S1). Enrichment of gene sets in cKO relative to WT T_{FH} cells were determined by GSEA. Positive enrichment scores (ES) indicate enrichment in cKO T_{FH} cells; negative ES indicates enrichment in WT T_{FH} cells. (B) Enrichment of gene sets related to branched chain amino acid degradation, fatty acid metabolism, and citrate cycle in cKO T_{FH} relative to WT T_{FH} cells determined by GSEA using KEGG curated pathway database. (C–F) Experiments were set up as Figure 4A. (C) Comparison of mitochondrial mass between day 8 WT T_{FH} (CXCR5^{high} SLAM^{low} solid line) and WT Th1 (CXCR5^{low} SLAM^{high} shaded) SMARTA cells, as determined by MitoTracker® Green FM. (D) Mitochondrial mass of day 8 T_{FH} and Th1 cKO (red) and WT (blue) SMARTA cells. (E) Mitochondrial membrane potential of day 8 WT T_{FH} (solid line) and WT Th1 (shaded) SMARTA cells, as determined by the MFI of DiOC6(3) staining. (F) Mitochondrial membrane potential of day 8 T_{FH} and Th1 cKO (red) and WT (blue) SMARTA cells. Data in (C–F) are from single experiments (n=5) representative of 2 independent experiments. Statistical significance in (C–F) was determined by paired t tests. Each line represents data from a single mouse.

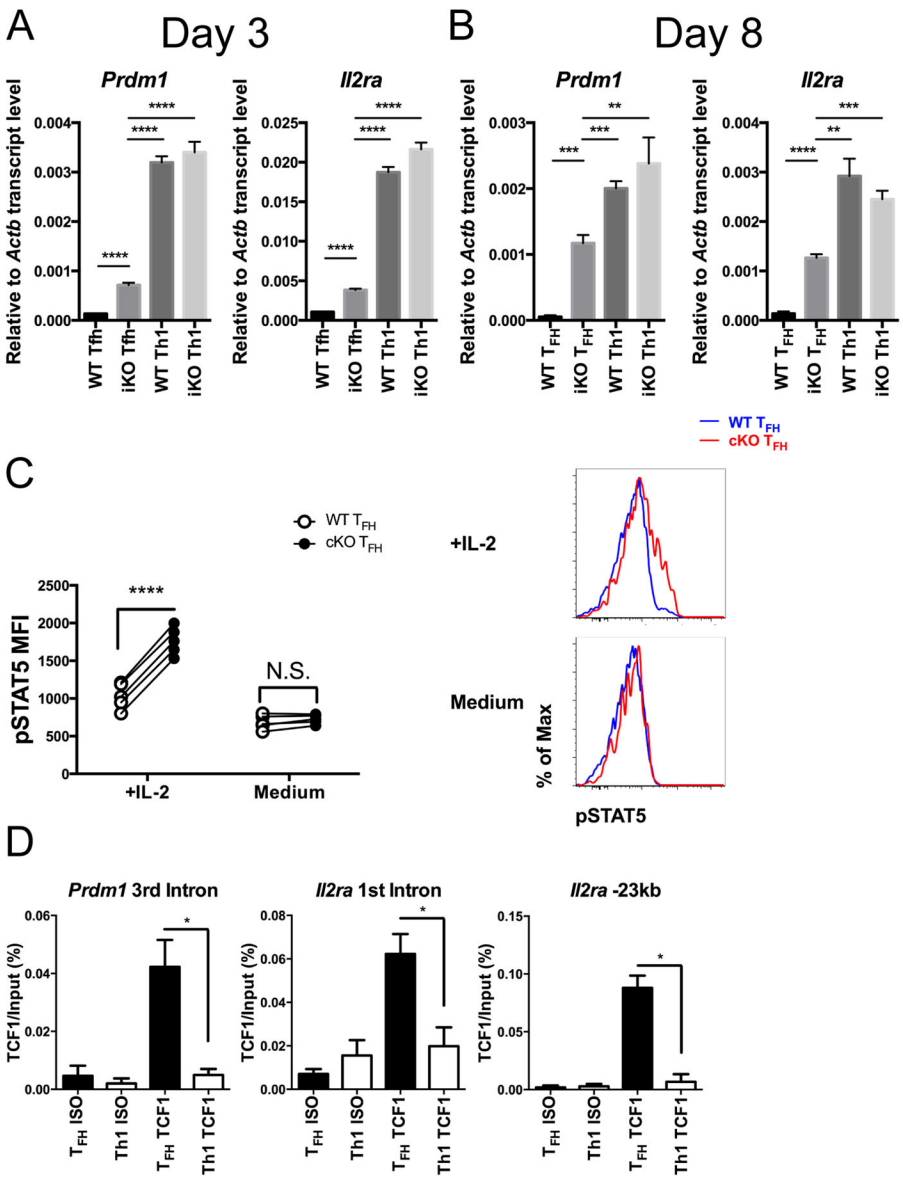

Figure 6. TCF1 suppresses the expression of *Prdm1 and Il2ra*

(A, B) QRT-PCR analyses of mRNA levels of *Prdm1* and *Il2ra* in sorted day 3 (A) or day 8 (B) T_{FH} and Th1 iKO and WT SMARTA cells, normalized to the mRNA levels of *Actb*. Data are from a single experiment representative of 2 independent experiments, set up as in Figure 4F and S4G. Statistical significance determined by an unpaired t test; error bars represent SD. (C) 10^4 purified CD4 T cells from cKO ($CD45.1^-CD45.2^+$) and WT ($CD45.1^+CD45.2^+$) SMARTA mice were mixed at ~1:1 ratio and adoptively transferred into each recipient, which were then infected with LCMV. On day 5 p.i., splenocytes were collected, cultured with or without 50U/mL human rIL-2 for 20min at 37°C and MFI of pSTAT5 in T_{FH} cKO and WT SMARTA determined. Data are from a single experiment (n=5) representative of 2 independent experiments. Significance was determined by a paired t test. (D) ChIP from day 8 T_{FH} and Th1 SMARTA cells using antibodies to TCF1 or

control IgG and amplified by QRT-PCR for the indicated regions (the third intron of *Prdm1*, the first intron of *Il2ra*, and −23kb from *Il2ra* TSS). Data are the mean +/− SEM of three independent experiments. Significance was determined by an unpaired t test.

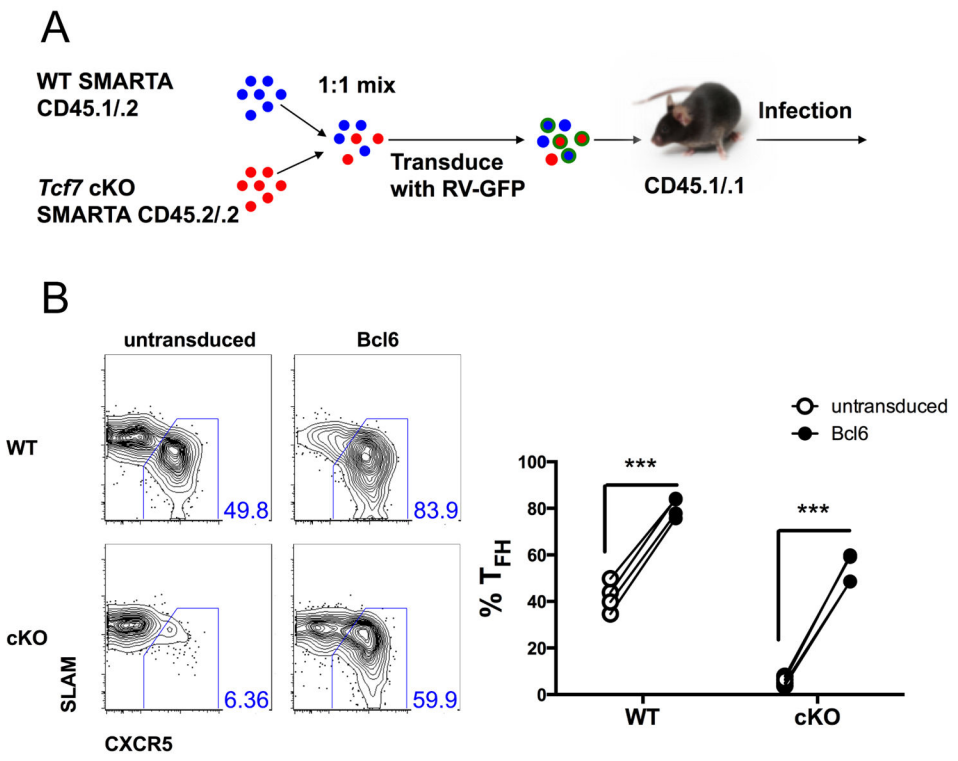

Figure 7. *Tcf7* deficiency is rescued by Bcl6 over-expression

(A) cKO and WT SMARTA CD4 T cells were mixed at ~1:1 ratio, transduced with retroviral constructs over-expressing Bcl6, and transferred into WT CD45.1 recipients (2×10^4 cells per recipient) that were then infected with LCMV. (B) Frequencies of T_{FH} within WT or cKO SMARTA cells untransduced or transduced with Bcl6 over-expression construct on day 8 p.i.. Data is from a single experiment representative of 2 independent experiments. Significance was determined by paired t tests.